

Spatially-varying meshless approximation method for enhanced computational efficiency

Mitja Jančič^{1,2}[0000–0003–1850–412X], Miha Rot^{1,2}[0000–0002–8869–4507], and
Gregor Kosec¹[0000–0002–6381–9078]

¹ Jožef Stefan Institute, Parallel and Distributed Systems Laboratory, Ljubljana,
Slovenia {mitja.jancic,miha.rot,gregor.kosec}@ijs.si

² Jožef Stefan International Postgraduate School, Ljubljana, Slovenia

Abstract. In this paper, we address a way to reduce the total computational cost of meshless approximation by reducing the required stencil size through spatial variation of computational node regularity. Rather than covering the entire domain with scattered nodes, only regions with geometric details are covered with scattered nodes, while the rest of the domain is discretised with regular nodes. Consequently, in regions covered with regular nodes the approximation using solely the monomial basis can be performed, effectively reducing the required stencil size compared to the approximation on scattered nodes where a set of polyharmonic splines is added to ensure convergent behaviour. The performance of the proposed hybrid scattered-regular approximation approach, in terms of computational efficiency and accuracy of the numerical solution, is studied on natural convection driven fluid flow problems. We start with the solution of the de Vahl Davis benchmark case, defined on square domain, and continue with two- and three-dimensional irregularly shaped domains. We show that the spatial variation of the two approximation methods can significantly reduce the computational complexity, with only a minor impact on the solution accuracy.

Keywords: Collocation · RBF-FD · RBF · Meshless · Hybrid method · Fluid-flow · Natural convection · Numerical simulation

1 Introduction

Although the meshless methods are formulated without any restrictions regarding the node layouts, it is generally accepted that quasi-uniformly-spaced node sets improve the stability of meshless methods [25,14,13]. Nevertheless, even with quasi-uniform nodes generated with recently proposed node positioning algorithms [19,16,15], a sufficiently large stencil size is required for stable approximation. A stencil with $n = 2\binom{m+d}{m}$ nodes is recommended [1] for the Radial Basis Function-generated Finite differences (RBF-FD) [21] method in a d -dimensional domain. The method with a basis of Polyharmonic splines (PHS) and monomial augmentation up to a certain order m has been demonstrated with scattered nodes on several applications [18,8,22,26]. On the other hand, approximation on

regular nodes can be performed with considerably smaller stencil [11] ($n = 5$ in two-dimensional domain) using only monomial basis.

Therefore, a possible way to enhance the overall computational efficiency and consider the discretization-related error is to use regular nodes sufficiently far away from any geometric irregularities in the domain and scattered nodes in their vicinity. A similar approach, where the approximation method is spatially varied, has already been introduced, e.g., a hybrid FEM-meshless method [6] has been proposed to overcome the issues regarding the unstable Neumann boundary conditions in the context of meshless approximation. Moreover, the authors of [5,2] proposed a hybrid of Finite Difference (FD) method employed on conventional cartesian grid combined with meshless approximation on scattered nodes. These hybrid approaches are computationally very efficient, however, additional implementation-related burden is required on the transition from cartesian to scattered nodes [10], contrary to the objective of this paper relying solely on the framework of meshless methods.

In this paper we experiment with such *hybrid scattered-regular* method with spatially variable stencil size on solution of natural convection driven fluid flow cases. The solution procedure is first verified on the reference de Vahl Davis case, followed by a demonstration on two- and three-dimensional irregular domains. We show that spatially varying the approximation method can have positive effects on the computational efficiency while maintaining the accuracy of the numerical solution.

2 Numerical treatment of partial differential equations

To obtain the hybrid scattered-regular domain discretization, we first fill the entire domain with regular nodes. A portion of this regular nodes are then removed in the areas where scattered node placement is desired, i.e., close to the irregular boundaries. Finally, the voids are filled with a dedicated node positioning algorithm [19] that supports variable nodal density and allows us to refine the solution near irregularities in the domain. This approach is rather naive but sufficient for demonstration purposes. A special hybrid fill algorithm is left for future work.

An example of an h -refined domain discretization is shown in Fig. 1. It is worth noting that the width of the scattered node layer δ_h is non-trivial and affects both the stability of the solution procedure and the accuracy of the numerical solution. Although we provide a superficial analysis of δ_h variation in Sections 4.1 and 4.2, further work is warranted.

After the computational nodes $\mathbf{x}_i \in \Omega$ are obtained, the differential operators can be approximated in point \mathbf{x}_c over a set of n neighbouring nodes (stencil) $\{\mathbf{x}_i\}_{i=1}^n = \mathcal{N}$, using the following expression

$$(u)(\mathbf{x}_c) \approx \sum_{i=1}^n w_i u(\mathbf{x}_i). \quad (1)$$

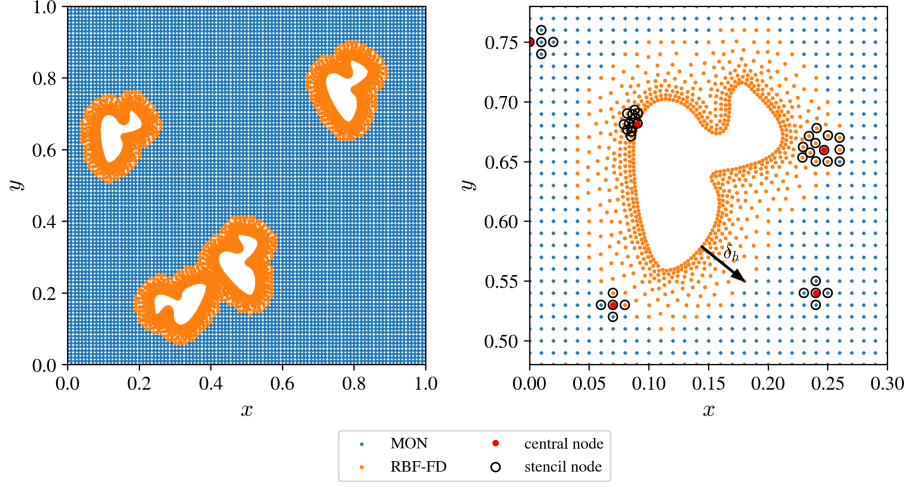


Fig. 1. Irregular domain discretization example (left) and spatial distribution of approximation methods along with corresponding example stencils (right).

The approximation (1) holds for an arbitrary function u and yet to be determined weights \mathbf{w} . To determine the weights, the equality of approximation (1) is enforced for a chosen set of basis functions. Here we will use two variants

- (i) a set of Polyharmonic splines (PHS) augmented with monomials to ensure convergent behaviour [7,1], effectively resulting in a popular *radial basis function-generated finite differences* (RBF-FD) approximation method [21].
- (ii) a set of monomials centred at the stencil nodes that we will refer to as (MON) [11].

We use the least expensive MON with $2d + 1$ monomial basis functions³ and the same number of support nodes in each approximation stencil. This setup is fast, but only stable on regular nodes [11,17]. For the RBF-FD part, we also resort to the minimal configuration required for 2nd-order operators, i.e., 3rd-order PHS augmented with all monomials up to the 2nd-order. According to standard recommendations [1], this requires a stencil size of $n = 2^{\binom{m+d}{m}}$.

Note the significant difference between stencil sizes – 5 vs. 12 nodes in 2D – that only increases in higher dimensions (7 vs. 30 in 3D). This results both in faster computation of the weights \mathbf{w} – an $\mathcal{O}(n^3)$ operation performed only once for each stencil – and in faster evaluation for the explicit operator approximation (1) performed many times during the explicit time stepping.

³ In 2D, the 5 basis functions are $\{1, x, y, x^2, y^2\}$.

2.1 Implementation details

The entire solution procedure employing hybrid scattered-regular method is implemented in C++. The projects implementation⁴ is strongly dependent on our in-house developed meshless C++ framework *Medusa library* [20] supporting all building blocks of the solution procedure, i.e., differential operator approximations, node positioning algorithms, etc.

We used `g++ 11.3.0` for Linux to compile the code with `-O3 -DNDEBUG` flags on Intel(R) Xeon(R) CPU E5520 computer. To improve the timing accuracy we run the otherwise parallel code in a single thread with the CPU frequency fixed at 2.27 GHz, disabled boost functionality and assured CPU affinity using the `taskset` command. Post-processing was done using Python 3.10.6 and Jupyter notebooks, also available in the provided git repository.

3 Governing problem

To further assess the advantages of the hybrid method, we focus on natural convection problem that is governed by a system of three PDEs describing the continuity of mass, the conservation of momentum and the transfer of heat

$$\nabla \cdot \mathbf{v} = 0, \quad (2)$$

$$\frac{\partial \mathbf{v}}{\partial t} + \mathbf{v} \cdot \nabla \mathbf{v} = -\nabla p + \nabla \cdot (Pr \nabla \mathbf{v}) - Ra Pr g T_{\Delta}, \quad (3)$$

$$\frac{\partial T}{\partial t} + \mathbf{v} \cdot \nabla T = \nabla \cdot (\nabla T), \quad (4)$$

where dimensionless nomenclature using Rayleigh (Ra) and Prandtl (Pr) numbers is used [24,12].

The temporal discretization of the governing equations is solved with explicit Euler time stepping where we first update the velocity using the previous step temperature field in the Boussinesq term [23]. The pressure-velocity coupling is performed using the Chorin's projection method [3] under the premise that the pressure term of the Navier-Stokes equation can be treated separately from other forces and used to impose the incompressibility condition. The time step is a function of internodal spacing h , and is defined as $dt = 0.1 \frac{h^2}{2}$ to assure stability.

4 Numerical results

4.1 The de Vahl Davis problem

First, we solve the standard de Vahl Davis benchmark problem [24]. The main purpose of solving this problem is to establish confidence in the presented solution procedure and to shed some light on the behaviour of considered approximation methods, the stability of the solution procedure and finally on the

⁴ Source code is available at gitlab.com/e62Lab/public/2023_cp_iccs_hybrid_nodes under tag *v1.0*.

computational efficiency. Furthermore, the de Vahl Davis problem was chosen as the basic test case, because the regularity of the domain shape allows us to efficiently discretize it using exclusively scattered or regular nodes and compare the solutions to that obtained with the hybrid scattered-regular discretization.

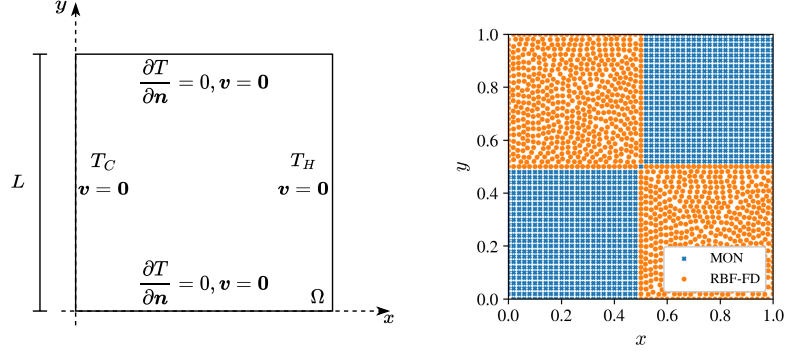


Fig. 2. The de Vahl Davis sketch (left) and example hybrid scattered-regular domain discretization (right).

For a schematic representation of the problem, see Fig. 2 (left). The domain is a unit box $\Omega = [0, 1] \times [0, 1]$, where the left wall is kept at a constant temperature $T_C = -0.5$, while the right wall is kept at a higher constant temperature $T_H = 0.5$. The upper and lower boundaries are insulated, and no-slip boundary condition for velocity is imposed on all walls. Both the velocity and temperature fields are initially set to zero.

To test the performance of the proposed hybrid scattered-regular approximation method, we divide the domain Ω into quarters, where each quarter is discretized either using scatter or regular nodes – see Fig. 2 (right) for clarity.

An example solution for $Ra = 10^6$ and $Pr = 0.71$ at a dimensionless time $t = 0.15$ with approximately $N = 15\,800$ discretization nodes is shown in Fig. 3.

We use the Nusselt number — the ratio between convective and conductive heat transfer — to determine when the steady state has been reached and as a convenient scalar value for comparison with reference solutions. In the following analyses, the average Nusselt number (\overline{Nu}) is calculated as the average of the Nusselt values at the cold wall nodes

$$Nu = \frac{L}{T_H - T_C} \left| \frac{\partial T}{\partial \mathbf{n}} \right|_{x=0}. \quad (5)$$

Its evolution over time is shown in Fig. 4. In addition, three reference results are also added to the figure. We are pleased to see that our results are in good agreement with the references from the literature.

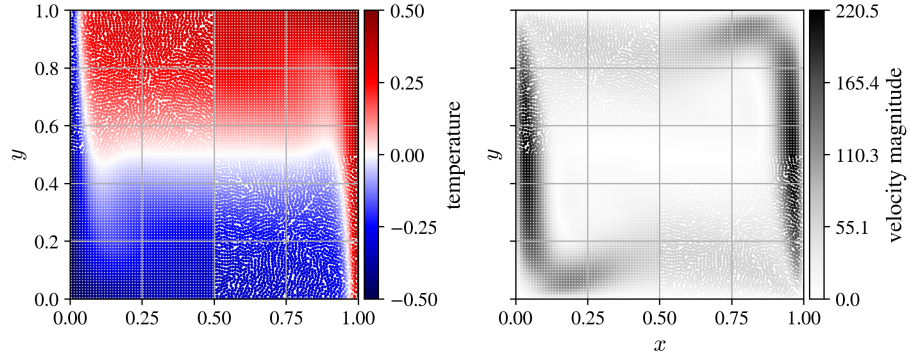


Fig. 3. Example solution at the stationary state. Temperature field (left) and velocity magnitude (right).

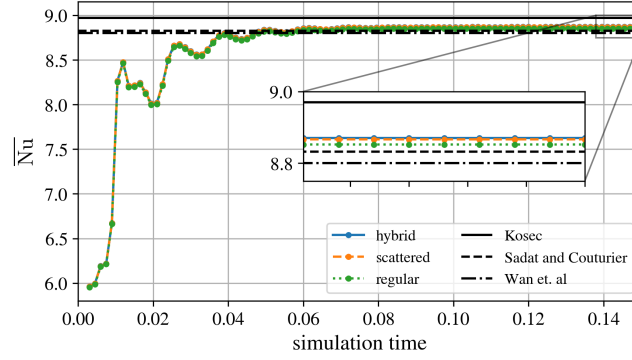


Fig. 4. Time evolution of the average Nusselt number along the cold edge calculated with the densest considered discretization. Three reference results Kosec [12], Sadat and Couturier [9] and Wan et. al. [4] are also added.

Moreover, Fig. 4 also shows the time evolution of the average Nusselt number value for cases where the entire domain is discretized using either scatter or regular nodes. We find that all — hybrid, purely scattered and purely regular domain discretizations — yield results in good agreement with the references. More importantly, the hybrid method shows significantly shorter computational times (about 50%) than that required by the scattered discretization employing RBF-FD, as can be seen in Tab. 1.

Approximation	$\overline{\text{Nu}}$	execution time [h]	N
scattered	8.867	6.23	55 477
regular	8.852	2.42	64 005
hybrid	8.870	3.11	59 694
Kosec (2007) [12]	8.97	/	10201
Sadat and Couturier (2000) [9]	8.828	/	22801
Wan et al. (2001) [4]	8.8	/	10201

Table 1. Average Nusselt along the cold edge along with execution times.

To further validate the hybrid method, we show in Fig. 5 the vertical component of the velocity field across the section $y = 0.5$. It is important to observe that the results for the hybrid, scattered and regular approaches overlap, which means that the resulting velocity fields for the three approaches are indeed comparable.

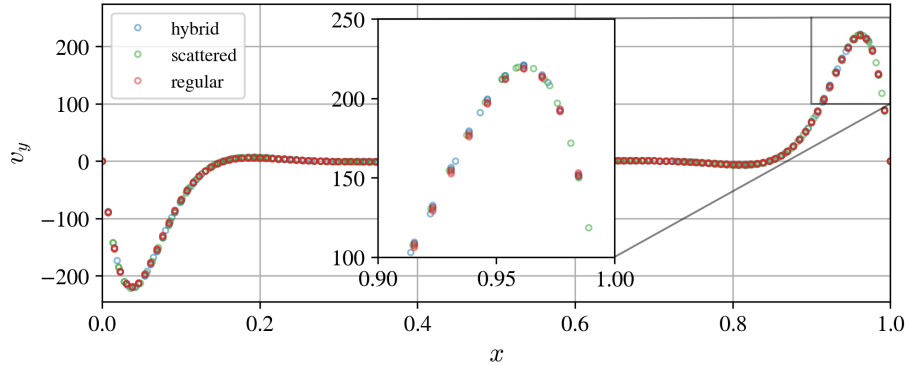


Fig. 5. Vertical velocity component values at nodes close to the vertical midpoint of the domain, i.e., $|y - 0.5| \leq h$ for purely scattered, purely regular and hybrid discretizations.

As a final remark, we also study the convergence of the average Nusselt number with respect to the number of discretization nodes in Fig. 6, where

we confirm that all our discretization strategies converge to a similar value, consistent with the reference values. Moreover, to evaluate the computational efficiency of the hybrid approach, the execution times are shown on the right. Note that the same values for h were used for all discretization strategies and the difference in the total number of nodes is caused by the lower density of scattered nodes at the same internodal distance.

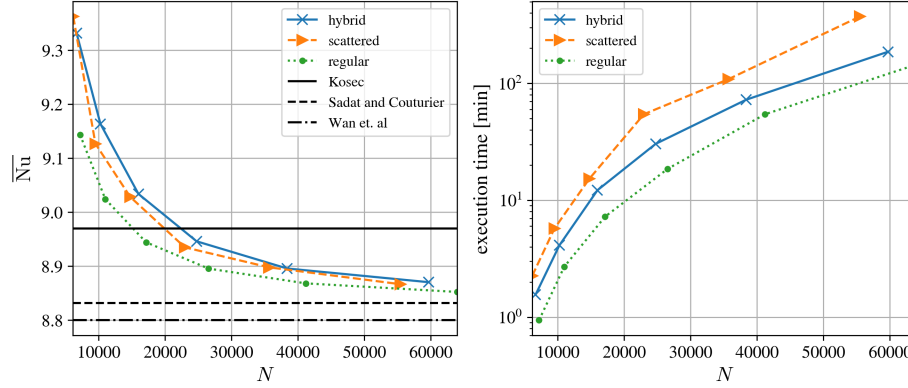


Fig. 6. Convergence of average Nusselt number with respect to discretization quality (left) and corresponding execution times (right).

The effect of the scattered nodes layer width δ_h To study the effect of the width of the scattered node layer δ_h , we consider two cases. In both cases, the domain from Fig. 2 is split into two parts at a distance $h\delta_h$ from the origin in the lower left corner. In the first scenario, the split is horizontal, resulting in scattered nodes below the imaginary split and regular nodes above it. In the second scenario, the split is vertical, resulting in scattered nodes to the left of it and regular nodes to the right of it. In both cases, the domain is discretized with purely regular nodes when $h\delta_h = 0$ and with purely scattered nodes when $h\delta_h = L$.

In Fig. 7, we show how the width of the scattered node layer affects the average Nusselt number in stationary state for approximately 40 000 discretization nodes. It is clear that even the smallest values of δ_h yield satisfying results. However, it is interesting to observe that the accuracy is significantly affected when the boundary between regular and scattered nodes runs across the region with the largest velocity magnitudes, i.e., the first and last couple of vertical split data points in Fig. 7.

4.2 Natural convection on irregularly shaped domains

In the previous section we demonstrated that the hybrid scattered-regular approximation method is computationally more efficient than the pure RBF-FD ap-

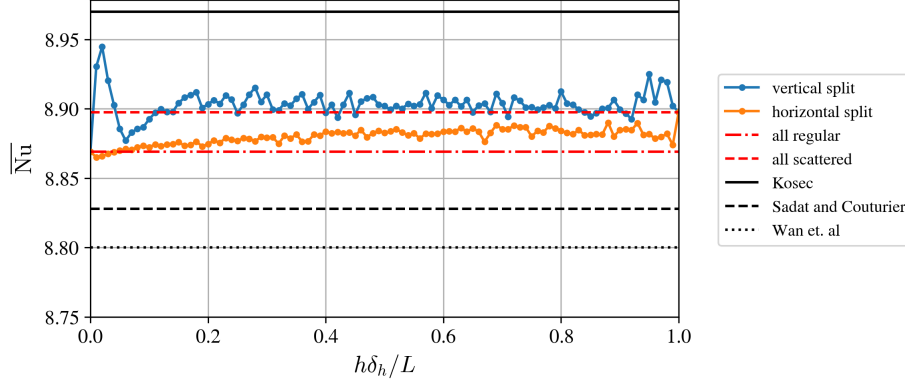


Fig. 7. Demonstration of the scattered node layer width (δ_h) effect on the accuracy of the numerical solution.

proximation. However, to truly exploit the advantages of the hybrid method, irregular domains must be studied. Therefore, in this section, the hybrid scattered-regular approach is employed on an irregularly shaped domain. Let the computational domain Ω be a difference between the two-dimensional unit box $\Omega = [0, 1] \times [0, 1]$ and 4 randomly positioned duck-shaped obstacles introducing the domain irregularity.

The dynamics of the problem is governed by the same set of equations (2-4) as in the previous section. This time, however, all the boundaries of the box are insulated. The obstacles, on the other hand, are subject to Dirichlet boundary conditions, with half of them at $T_C = 0$ and the other half at $T_H = 1$. The initial temperature is set to $T_{\text{init}} = 0$.

We have chosen such a problem because it allows us to further explore the advantages of the proposed hybrid scattered-regular discretization. Generally speaking, the duck-shaped obstacles within the computational domain present an arbitrarily complex shape, requiring scattered nodes to accurately describe them and reduce the discretization-related errors. Moreover, by using scattered nodes near the irregularly shaped domain boundaries, we can further improve the local field description in their vicinity by employing the h -refinement. Specifically, we employ h -refinement towards the obstacles with linearly decreasing internodal distance from $h_r = 0.01$ (regular nodes) towards $h_s = h_r/3$ (irregular boundary) over a distance of $h_r\delta_h$. The refinement distance and the width of the scattered node layer are the same, except in the case of fully scattered discretization. Such setup effectively resulted in approximately $N = 11\,600$ computational nodes ($N_s = 3149$ scattered nodes and $N_r = 8507$ regular nodes), as shown in Fig. 1 for a scattered node layer width $\delta_h = 4$. Note that the time step is based on the smallest h , i.e., $dt = 0.1 \frac{h_s^2}{2}$.

Fig. 8 (left) shows an example solution for an irregularly shaped domain. The hybrid scattered-regular solution procedure was again able to obtain a reasonable numerical solution.

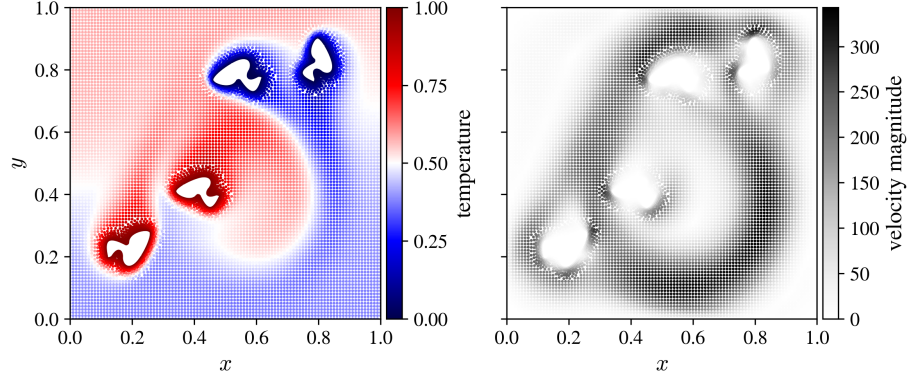


Fig. 8. Example solution on irregular domain. Temperature field (left) and velocity magnitude (right).

Furthermore, Fig. 9 shows the average Nusselt number along the cold duck edges where we can observe that a stationary state has been reached. The steady state values for all considered discretizations match closely but it is interesting to note that in the early stage of flow formation, the fully scattered solutions with different refinement distance δ_h differ significantly more than the hybrid and the fully scattered solutions with the same refinement strategy.

It is perhaps more important to note that the execution times were 46 and 29 minutes for purely scattered and hybrid discretizations respectively (both with nodal density refinement over $\delta_h = 4$), effectively reducing the execution time for approximately 35 %, while no numerical solution could be obtained for the pure regular discretisation with MON approximation.

The effect of the scattered nodes layer width δ_h To justify the use of $\delta_h = 4$, we show in Fig. 8 (right) the average value of the Nusselt number at steady state for different values of δ_h . In the worst case, the difference is $< 2\%$, justifying the use of the computationally cheaper smaller δ_h . Note that in this particular domain setup, $\delta_h > 64$ already yields a purely scattered domain discretization, while the minimum working value is $\delta_h = 4$. Note also that the general increase of the Nusselt number with respect to the width of the scattered node layers δ_h may also exhibit other confounding factors. An increase in δ_h leads to a finer domain discretization due to the more gradual refinement, i.e., in a fully scattered discretization using $\delta_h = 70$ results in about 35 000 discretization points compared to 11 600 at $\delta_h = 4$, and the aggressiveness of the refinement

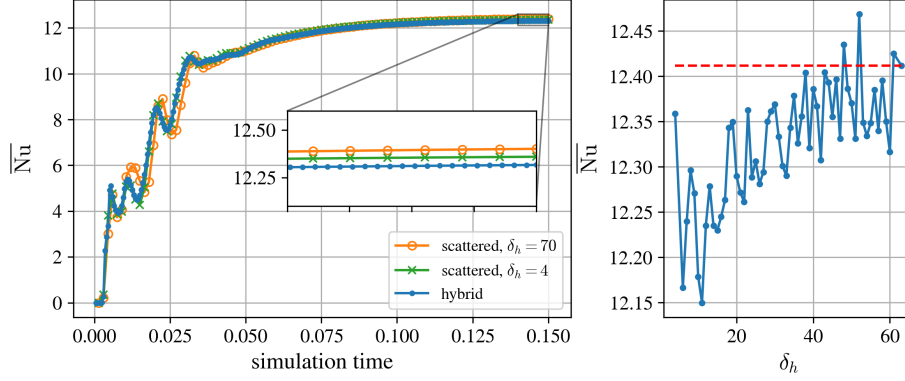


Fig. 9. Time evolution of the average Nusselt number calculated on the cold duck-shaped obstacles of an irregularly shaped domain.

could also play a role. This can be confirmed by observing the difference between the results for the two fully scattered discretizations in Fig. 9.

4.3 Application to three-dimensional irregular domains

As a final demonstrative example, we employ the proposed hybrid scattered-regular approximation method on a three-dimensional irregular domain. The computational domain Ω is a difference between the three-dimensional unit box $\Omega = [0, 1] \times [0, 1] \times [0, 1]$ and 4 randomly positioned and sized spheres introducing the domain irregularity.

The dynamics is governed by the same set of equations (2-4) as in the two-dimensional case from Sect. 4.2. To improve the quality of the local field description near the irregularly shaped domain boundaries, the h -refinement is employed with a linearly decreasing internodal distance from $h_r = 0.025$ (regular nodes) towards $h_s = h_r/2$ (spherical boundaries). Two spheres were set to a constant temperature $T_C = 0$ and the remaining two to $T_H = 1$. The Rayleigh number was set to 10^4 .

Although difficult to visualize, an example solution is shown in Fig. 10. Using the hybrid scattered-regular domain discretization, the solution procedure was again able to obtain a reasonable numerical solution.

Note that the scattered method took about 48.2 hours and the hybrid scattered-regular approximation method took 20.5 hours to simulate 1 dimensionless time unit with the dimensionless time step $dt = 7.8125 \cdot 10^{-6}$ and about 75 000 computational nodes with $\delta_h = 4$.

5 Conclusions

We proposed a computationally efficient approach to the numerical treatment of problems in which most of the domain can be efficiently discretized with reg-

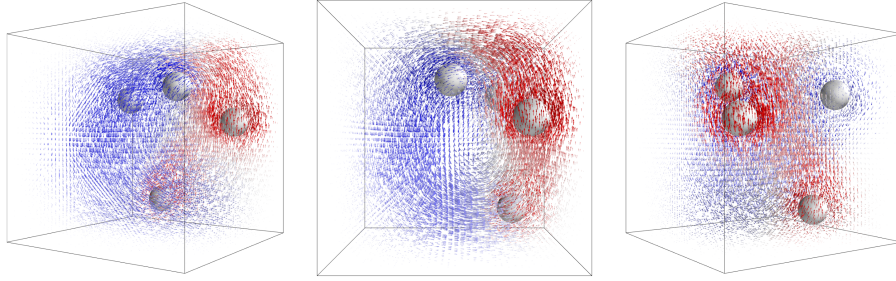


Fig. 10. Example solution viewed from three different angles. The arrows show the velocity in computational nodes and are coloured according to the temperature in that node. The values range from dark blue for T_C to dark red for T_H . For clarity, only $\frac{1}{3}$ of the nodes are visualized.

ularly positioned nodes, while scattered nodes are used near irregularly shaped domain boundaries to reduce the discretization-related errors. The computational effectiveness of the spatially-varying approximation method, employing FD-like approximation on regular nodes and RBF-FD on scattered nodes, is demonstrated on a solution to a two-dimensional de Vahl Davis natural convection problem.

We show that the proposed hybrid method, can significantly improve the computational efficiency compared to the pure RBF-FD approximation, while introducing minimal cost to the accuracy of the numerical solution.

In the continuation, the hybrid method is applied to a more general natural convection problem in two- and three-dimensional irregular domains, where the elegant mathematical formulation of the meshless methods is further exposed by introducing h -refinement towards the irregularly shaped obstacles. In both cases, the hybrid method successfully obtained the numerical solution and proved to be computationally efficient, with execution time gains nearing 50 %.

Nevertheless, the scattered node layer width and the aggressiveness of h -refinement near the irregularly shaped domain boundaries should be further investigated, as both affect both the computational efficiency and stability of the solution procedure. In addition, future work should also include more difficult problems, such as mixed convection problems and a detailed analysis of possible surface effects, e.g. scattering, at the transition layer between the scattered and regular domains.

Acknowledgements The authors would like to acknowledge the financial support of Slovenian Research Agency (ARRS) in the framework of the research core funding No. P2-0095, the Young Researcher program PR-10468 and research project J2-3048.

Conflict of interest The authors declare that they have no conflict of interest. All the co-authors have confirmed to know the submission of the manuscript by the corresponding author.

References

1. Bayona, V., Flyer, N., Fornberg, B., Barnett, G.A.: On the role of polynomials in rbf-fd approximations: Ii. numerical solution of elliptic pdes. *Journal of Computational Physics* **332**, 257–273 (2017)
2. Bourantas, G., Mountris, K., Loukopoulos, V., Lavier, L., Joldes, G., Wittek, A., Miller, K.: Strong-form approach to elasticity: Hybrid finite difference-meshless collocation method (fdmcm). *Applied Mathematical Modelling* **57**, 316–338 (2018). <https://doi.org/https://doi.org/10.1016/j.apm.2017.09.028>
3. Chorin, A.J.: Numerical solution of the navier-stokes equations. *Mathematics of computation* **22**(104), 745–762 (1968)
4. D. C. Wan, B. S. V. Patnaik, G.W.W.: A new benchmark quality solution for the buoyancy-driven cavity by discrete singular convolution. *Numerical Heat Transfer, Part B: Fundamentals* **40**(3), 199–228 (2001). <https://doi.org/10.1080/104077901752379620>, <https://doi.org/10.1080/104077901752379620>
5. Ding, H., Shu, C., Yeo, K., Xu, D.: Simulation of incompressible viscous flows past a circular cylinder by hybrid fd scheme and meshless least square-based finite difference method. *Computer Methods in Applied Mechanics and Engineering* **193**(9–11), 727–744 (2004)
6. El Kadmiri, R., Belaasilia, Y., Timesli, A., Kadiri, M.S.: A hybrid algorithm using the fem-meshless method to solve nonlinear structural problems. *Engineering Analysis with Boundary Elements* **140**, 531–543 (2022). <https://doi.org/https://doi.org/10.1016/j.enganabound.2022.04.018>
7. Flyer, N., Fornberg, B., Bayona, V., Barnett, G.A.: On the role of polynomials in rbf-fd approximations: I. interpolation and accuracy. *Journal of Computational Physics* **321**, 21–38 (2016)
8. Fornberg, B., Flyer, N.: A primer on radial basis functions with applications to the geosciences. SIAM (2015)
9. H. Sadat, S.C.: Performance and accuracy of a meshless method for laminar natural convection. *Numerical Heat Transfer, Part B: Fundamentals* **37**(4), 455–467 (2000). <https://doi.org/10.1080/10407790050051146>, <https://doi.org/10.1080/10407790050051146>
10. Javed, A., Djidjeli, K., Xing, J., Cox, S.: A hybrid mesh free local rbf-cartesian fd scheme for incompressible flow around solid bodies. *International Journal of Mathematical, Computational, Natural and Physical Engineering* **7**, 957–966 (2013)
11. Kosec, G.: A local numerical solution of a fluid-flow problem on an irregular domain. *Advances in engineering software* **120**, 36–44 (2018)
12. Kosec, G., Šarler, B.: Solution of thermo-fluid problems by collocation with local pressure correction. *International Journal of Numerical Methods for Heat & Fluid Flow* (2008)
13. Liu, G.R.: Meshfree methods: moving beyond the finite element method. CRC press (2009)
14. Patel, V.G., Rachchh, N.V.: Meshless method–review on recent developments. *Materials today: proceedings* **26**, 1598–1603 (2020)

15. van der Sande, K., Fornberg, B.: Fast variable density 3-d node generation. *SIAM Journal on Scientific Computing* **43**(1), A242–A257 (2021)
16. Shankar, V., Kirby, R.M., Fogelson, A.L.: Robust node generation for meshfree discretizations on irregular domains and surfaces. *SIAM J. Sci. Comput.* **40**(4), 2584–2608 (2018). <https://doi.org/10.1137/17m114090x>
17. Slak, J., Kosec, G.: Refined meshless local strong form solution of cauchy–navier equation on an irregular domain. *Engineering Analysis with Boundary Elements* **100**, 3–13 (2019). <https://doi.org/https://doi.org/10.1016/j.enganabound.2018.01.001>, improved Localized and Hybrid Meshless Methods - Part 1
18. Slak, J., Kosec, G.: Adaptive radial basis function-generated finite differences method for contact problems. *International Journal for Numerical Methods in Engineering* **119**(7), 661–686 (Aug 2019). <https://doi.org/10.1002/nme.6067>
19. Slak, J., Kosec, G.: On generation of node distributions for meshless pde discretizations. *SIAM Journal on Scientific Computing* **41**(5), A3202–A3229 (2019)
20. Slak, J., Kosec, G.: Medusa: A c++ library for solving pdes using strong form mesh-free methods. *ACM Transactions on Mathematical Software (TOMS)* **47**(3), 1–25 (2021)
21. Tolstykh, A., Shirobokov, D.: On using radial basis functions in a “finite difference mode” with applications to elasticity problems. *Computational Mechanics* **33**(1), 68–79 (2003)
22. Tóth, B., Düster, A.: h-adaptive radial basis function finite difference method for linear elasticity problems. *Computational Mechanics* **71**(3), 433–452 (2023)
23. Tritton, D.J.: *Physical Fluid Dynamics*. Oxford Science Publ, Clarendon Press (1988). <https://doi.org/https://doi.org/10.1007/978-94-009-9992-3>
24. de Vahl Davis, G.: Natural convection of air in a square cavity: a bench mark numerical solution. *International Journal for numerical methods in fluids* **3**(3), 249–264 (1983)
25. Wendland, H.: *Scattered data approximation*, vol. 17. Cambridge university press (2004)
26. Zamolo, R., Nobile, E.: Solution of incompressible fluid flow problems with heat transfer by means of an efficient rbf-fd meshless approach. *Numerical Heat Transfer, Part B: Fundamentals* **75**(1), 19–42 (2019)